

e-ISSN: 2149-3367

**Borate Glasses** 

## Afyon Kocatepe Üniversitesi Fen ve Mühendislik Bilimleri Dergisi

Afyon Kocatepe University - Journal of Science and Engineering

https://dergipark.org.tr/tr/pub/akufemubid



Araştırma Makalesi / Research Article DOI: https://doi.org/10.35414/akufemubid.1602154

AKU J. Sci. Eng. 25 (2025) 051103 (1040-1052)

## **Computational Study of Radiation Shielding** Characteristics for Nd<sup>+3</sup> Doped Al<sub>2</sub>O<sub>3</sub>-Na<sub>2</sub>O-WO<sub>3</sub>-B<sub>2</sub>O<sub>3</sub>

\*Makale Bilgisi / Article Info Alındı/Received: 16.12.2024 Kabul/Accepted: 02.05.2025 Yayımlandı/Published: 01.10.2025

Nd<sup>+3</sup> Katkılı Al<sub>2</sub>O<sub>3</sub>–Na<sub>2</sub>O–WO<sub>3</sub>–B<sub>2</sub>O<sub>3</sub> Borat Camları İçin Radyasyon Zırhlama Özelliklerinin Hesaplamalı Çalışması

Zeynep AYGUN<sup>2\*</sup>, Murat AYGUN<sup>1</sup>

AKÜ FEMÜBİD 25 (2025) 051103 (1040-1052)

<sup>1</sup> Bitlis Eren University, Faculty of Science and Arts, Physics Department, Bitlis, Türkiye



© 2025 The Authors | Creative Commons Attribution-Noncommercial 4.0 (CC BY-NC) International License

### Öz

Nd<sub>2</sub>O<sub>3</sub> doped Al<sub>2</sub>O<sub>3</sub>-Na<sub>2</sub>O-WO<sub>3</sub>-B<sub>2</sub>O<sub>3</sub> glasses which were produced by melt quenching technique was studied for determining their charged particle, neutron and gamma-ray shielding characteristics. In this context, the radiationattenuating parameters were calculated by the help of PENELOPE, Phy-X/PSD, SRIM and PAGEX codes. The effect of neodymium on the glasses were evaluated and compared comprehensively. The results demonstrated a linear correlation between the shielding efficiencies of charged particles specifically alpha, electron, proton particles; gamma rays; and neutrons - and the neodymium content present in the samples. The glasses with the higher content of neodymium displayed better protection potential. The order of mass stopping power results of the glasses were found for the charged particles as MSPalpha > MSPprotons > MSPpositrons > MSPelectrons. The glass without Nd composition showed maximal range values for charged particles, whereas the glass with higher Nd composition demonstrated the minimal values. The largest stopping time values were obtained in the following order: Stpositron > Stelectron. The biggest stopping time value was observed for the glass without Nd. The glass with higher Nd exhibits the highest fast neutron attenuation. It can be posited that each of the glasses in question could be employed as shields in various application fields.

Keywords Gamma shielding; Charged particle attenuating; Neutron attenuating; Borate glass; Nd.

## 1. Introduction

It is of great importance to consider that medical personnel involved in radiation-based procedures such as fluoroscopy, mammography, tomosynthesis and computed tomography occupational radiation exposure. Those engaged in the performance of these procedures are confronted with the possibility of adverse health consequences resulting from exposure to ionizing radiation. It is critical to apply effective strategies to diminish the incidence of adverse effects of exposure to ionizing radiation for personnel working in imaging rooms used for radiological diagnosis and treatment methods.

#### **Abstract**

Eriyik söndürme tekniği ile üretilen Nd<sub>2</sub>O<sub>3</sub> katkılı Al<sub>2</sub>O<sub>3</sub>-Na<sub>2</sub>O-WO<sub>3</sub>-B<sub>2</sub>O<sub>3</sub> camlarının yüklü parçacık, nötron ve gama ışını zırhlama özelliklerinin belirlenmesi amaçlanmıştır. Bu bağlamda, radyasyon zayıflatma parametreleri PENELOPE, Phy-X/PSD, ve PAGEX kodları yardımıyla hesaplanmıştır. Neodimyumun camlar üzerindeki etkisi ayrıntılı olarak değerlendirilmiş ve kapsamlı bir şekilde karşılaştırılmıştır. Yüklü parçacık (alfa, proton ve elektron), gama ışını ve nötron zırhlama etkinliklerinin neodimyum içeriğiyle orantılı olduğu bulunmuştur. Daha yüksek neodimyum içeriğine sahip camlar daha iyi zayıflatma potansiyeli göstermiştir. Camların kütle durdurma gücü sonuçlarının sırası yüklü parçacıklar için MSPalfa > MSPprotonlar > MSPpozitronlar > MSPelektronlar olarak bulunmuştur. Nd bulunmayan cam, yüklü parçacıklar için maksimum değerleri gösterirken, daha yüksek Nd içeriği olan cam minimum değerleri göstermiştir. En büyük durdurma süresi değerleri şu sırayla elde edilmiştir: Stpozitron > Stelektron. En büyük durdurma süresi değeri Nd'siz cam için gözlenmiştir. Daha yüksek Nd'li cam en yüksek hızlı nötron zayıflamasını göstermiştir. Tüm camların birçok uygulama alanında zırhlama malzemesi olarak kullanılabileceği söylenebilir.

Anahtar Kelimeler Gama zırhlama; Yüklü parçacık zırhlama; Nötron zırhlama: Borat camı: Nd.

Glass is a substance of considerable importance to those engaged in scientific investigation, given the numerous advantageous characteristics it exhibits, comprising its exemplary corrosion resistance, hardness, optical characteristics, efficiency in light transmission, low thermal and electrical conductivity, low costs of production and versatility in processing through diverse techniques (Kaewnum et al., 2018; Yaacob et al., 2021; Aljewaw et al., 2022; Biradar et al., 2024, Nabil et al., 2024).

Due to the numerous advantages, it offers, glass is one of the most widely preferred and extensively analyzed

<sup>&</sup>lt;sup>2</sup> Bitlis Eren University, Vocational School of Technical Sciences, Bitlis, Türkiye

materials in the field of protecting against radiation (Alsafi et al., 2024; Yorulmaz et al., 2024; Alzahrani et al., 2024; Biradar et al., 2024; Nabil et al., 2024; Aygun, 2023; Karpuz, 2024). The transparency of glass represents a crucial advantage in its utilization within the field of radiation shielding. This quality enables the material to be suited to particular applications, including the fabrication of masks designed to safeguard the face and different parts of the face throughout the radiological procedures and the utilization of radiography rooms' fenestration and wall surfaces (Mhareb, 2024).

The rare earth element group is a material of great importance to a multitude of industries. These include glass, ceramics, alloy, the laser production, metallurgical industry, magnet production, high-tech devices, oil catalyst etc. (Kutu, 2024; Baykal et al. 2024; Aygun, 2024; Aygun et al., 2024; Charfi et al., 2024). The utilization of glass doped with rare earth elements (REEs) has become a fundamental aspect of the advancement of photonic applications in contemporary society. In recent past decades, a notable emphasis has been placed on the process of synthesising materials that have been doping with REs for incorporation into lighting technologies (Boussetta et al., 2024; Charfi et al., 2024; Gracie et al., 2024; Sivakumar et al., 2024; Lakshminarayana et al., 2020; Malchukova et al., 2018). Furthermore, it is crucial to investigate the impact of external ionizing radiation on the microstructure of glass structures. An understanding of the manner in which radiation interacts with glasses provides insight into how glassy matrices respond to radiation. Moreover, the combination of rare earth and transition metals with borosilicate results in the emergence of novel properties, including those concerned with absorption and emission. As a case in point, neodymium trioxide (Nd<sub>2</sub>O<sub>3</sub>) is a member of the rare earth element series. The neodymium (Nd3+) ion is employed extensively in a variety of materials, including as a dopant in solid-state lasers and for the generation of light. The optical properties of Nd<sup>3+</sup> have attracted the attention of scientists owing to the high level of its absorption range, which encompasses ultraviolet (UV) and near-infrared (NIR) wavelengths, and extensive cross section of emission, which optimizes laser pumping efficiency while maintaining energy levels conducive to high-gain host and low laser thresholds media (Abouhaswa and Taha, 2024; Mhareb, 2024; Matos and Balzaretti, 2024; Madhu et al., 2024). Neodymium (Nd) displays distinctive properties that are advantageous in the context of radiation shielding. Nd<sub>2</sub>O<sub>3</sub> exhibits relatively high density, which allows for greater radiation attenuation through increased interaction with incoming

radiation. It is noteworthy that neodymium exhibits a remarkable capacity to attenuate neutrons, including in its oxide form. Such characteristics are of paramount importance in nuclear technology, where the ability to absorb neutrons represents a critical capability (Mhareb, 2024). Tungsten oxide finds application in a number of fields, containing gamma radiation shielding, digital displays, optical recording systems, smart windows, and solid-state sensors for monitoring gas, temperature and humidity. Al2O3 has been found to enhance a number of properties, including electrical conductivity, mechanical strength, thermal stability, index of refraction and phonon energy. The motivation of this paper is to examine the characteristics of the interaction between radiation and glass. In order to achieve this, it is necessary to consider the radiation protection parameters (RPP), which are essential for understanding the attenuating abilities of the glasses in question. These include the linear and mass attenuation coefficient values (LACVs and MACVs), half value layer value (HVLV), mean free path value (MFPV), cross section of electron (ECS) and cross section of atom (ACS), conductivity and effective electron density (Ceff and Neff), effective atomic number (Zeff), buildup factors (BUF), equivalent atomic number (Zeq), μen/ρ, KERMA, the mass stopping power (MSP), fast neutron removal cross section value (FNRCSV), radiation yield (Ry), projected range (Rp) and stopping time (St). In this context, the RPP [(65-x) B2O3 - 5Al2O3 - 20Na2O -10WO3 - xNd2O3] (x =0, 0.25, 0.50, 0.75 mol%) glasses are evaluated by PENELOPE (Sempau et al., 2003), Phy-X/PSD (Sakar et al., 2020), SRIM (Ziegler) and PAGEX (Prabhu et al., 2021) codes for a variety of energy levels.

**Table 1.** The %mol ingredients and densities of the glasses (Attallah et al., 2024).

Sample	B2O3	Al203	Na2O	WO3	Nd2O3	Density (g/c
Nd1	65.00	5	20	10	0	2.56
Nd2	64.75	5	20	10	0.25	2.60
Nd3	64.50	5	20	10	0.50	2.62
Nd4	64.25	5	20	10	0.75	2.65

### 2. Materials and Methods

The data presented in this study regarding the glasses was obtained from Attallah et al., (2024) to examine the potential of these materials for radiation attenuation. The glass samples with a composition of [(65-x) B2O3 – 5Al2O3 - 20Na2O - 10WO3 - xNd2O3] x = zero, 0.25, 0.50 and 0.75 mol% were produced using the melt quenching technique. Table 1 illustrates the densities, molar volumes and chemical compositions of the selected glasses. The samples under examination are identified by the following labels: Nd1, Nd2, Nd3 and Nd4 for x = zero, 0.25, 0.50, and 0.75 mol%, respectively.

### 3. Results and Discussions

# 3.1. Analysis on the radiation attenuation properties of uncharged and charged particles

The variation of the MACVs versus energies is pictured in Figure 1(a). The MACVs demonstrated a pronounced decline as a consequence of the photoelectric (PE) in the low energy levels. In the mid-energy region, a minor alteration was observed due to Compton scattering (CS). As energy rises, there is an observable rise in the quantity of MACVs due to pair production (PP). It can be stated that the glasses provide effective protection, with Nd4 demonstrating slightly superior performance compared to other results. The glasses exhibited uniform shielding capabilities. Furthermore, the LACVs that are dependent on photon energies are illustrated in Fig. 1(b), and the similar protective characteristics were also observed in the glasses. The comparison of MACVs for the glasses and previously studied shielding materials; ordinary concrete (OC), steel-magnetite (Steel-magn.) (Bashter, 1997) are given in Fig. 2. It is obtained that the shielding capability depending on MAC results for the glasses are higher than the materials studied before particularly at energies below 1 MeV.

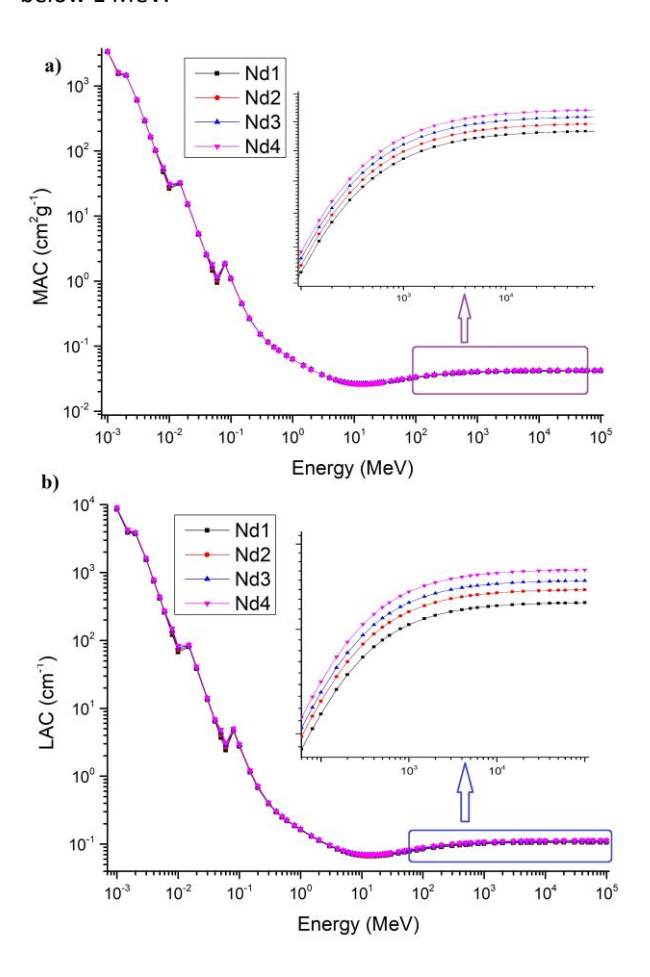
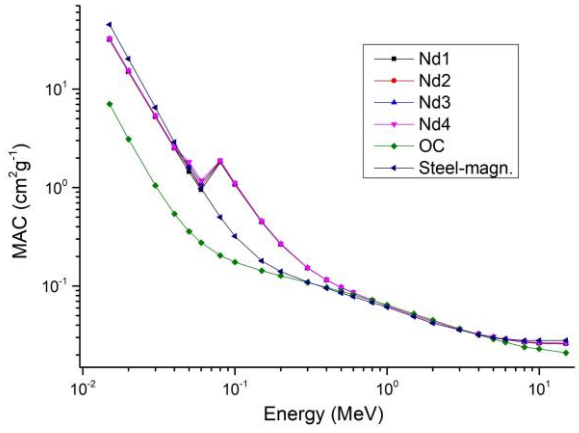
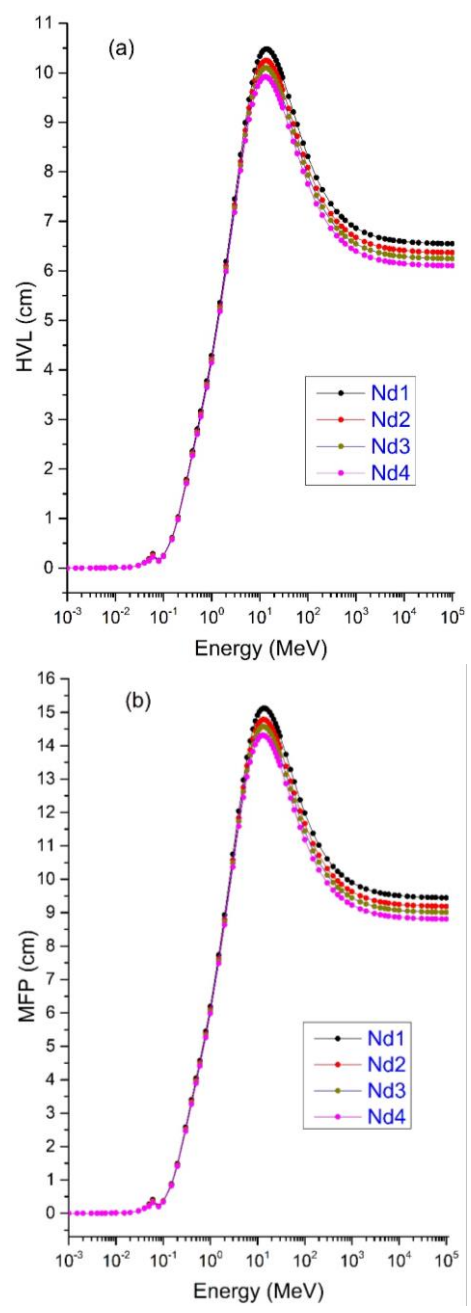


Figure 1. Changes of MACVs (a) and LACVs (b) versus energies.



**Figure 2.** The comparison of MACVs for the glasses and shielding materials studied before.



**Figure 3**. The changes of the values of the HVL (a) and MFP (b) versus energies.

The results obtained for the HVL and MFP are presented in Figures 3(a-b), respectively. At energies predominantly characterized by CS, it was noticed that photons demonstrated a markedly elevated probability of scattering. It was thus found that thicker materials were necessary, as they demonstrated a diminished potential for absorption and a higher MFP for photons. In the region of high energy, the obtained reduction in HVLVs and MFPVs was found to improve the protective characteristics. In the energy range of interest, it is essential to achieve lower values for both MFP and HVL, whereas in the lower energy region, thickness is a determining factor. The HVL and MFP results are in the order of Nd4 < Nd3 < Nd2 < Nd1. It is worthy of mention that glass Nd1 has the least shielding capability because of the high HVLVs and MFPVs, and Nd4 has the best shielding performance due to the lowest values. The comparison of HVLVs for the glasses and previously studied shielding materials (Bashter, 1997; Aygun and Aygun, 2023) is given in Fig. 4, and it is said that the glasses have higher protection ability than the materials.

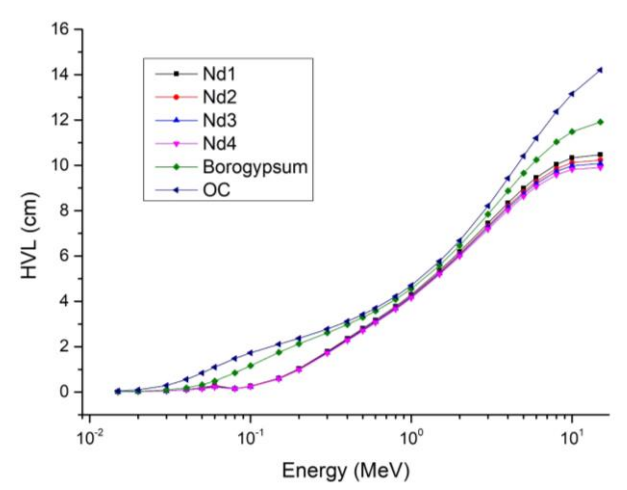


**Figure 4.** A comparative evaluation of HVLVs for the glasses and previously reported shielding materials.

It would be worthwhile to investigate the interaction probabilities of a material in greater depth, as illustrated by the ACS and ECS values presented in Figures 5(a-b), respectively. The findings indicate a correlation between the ACS and ECS values and photon energy. It may be inferred that the highest ACS and ECS results correspond to enhanced protection. Nd4 exhibits the most substantial protection characteristics among the glass samples, as evidenced by the ECS and ACS values.

The Zeff outcomes, as illustrated in Fig. 6(a), exhibited the gratest values due to the presence of PE at low energies. The findings demonstrated a distinct reduction and followed by an increase as the energy value increased, before reaching a level of stability at higher energies. It

was observed that glass compositions containing Nd in excess of 0.75% exhibited the highest Zeff values, thereby exhibiting the highest degree of attenuating potantials.

Conversely, the Nd1 composition, which contains a lower quantity of Nd, demonstrated the lowest Zeff values and the least effective protective capacity. The Zeg values are presented in Fig. 6(b). The data indicate that Nd4 exhibits greater degree of interaction, whereas demonstrates the least interaction between radiation and matter. It can be concluded from the presented values that Nd4 displays a more notable effect in response to radiation than Nd1, which evinces the weakest interaction between the glasses under examination. A comparative analysis of Zeff data for the glasses and a selection of earlier studies on shielding materials (Bashter, 1997) are given in Fig. 7. It is obtained that the shielding effect based on Zeff for the glasses under examination are of a greater extent than those materials previously documented especially at energies below 0.2 MeV.

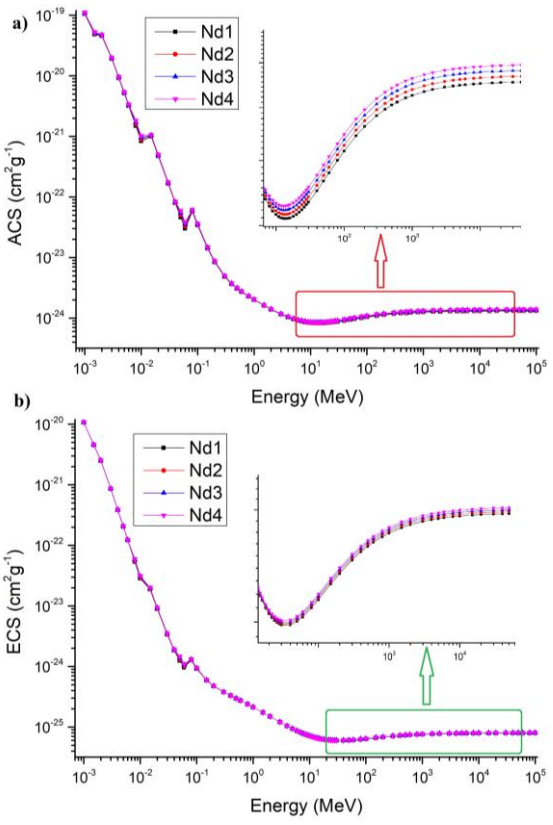


**Figure 5.** Dependence of the values for ACS (a) and ECS (b) versus energies.

Based on the PE, CS, and PP interactions, photon-matter interactions cause changes to the number of free electrons within the material. The nature of the change in question depends on the specific Neff results that are in accordance with the quantity of conduction electrons exist in the material in question.

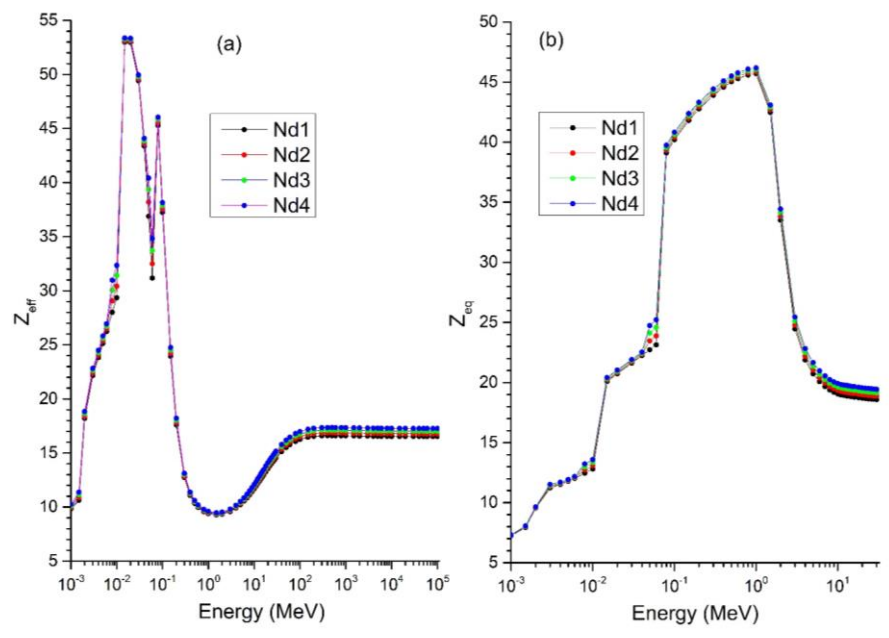
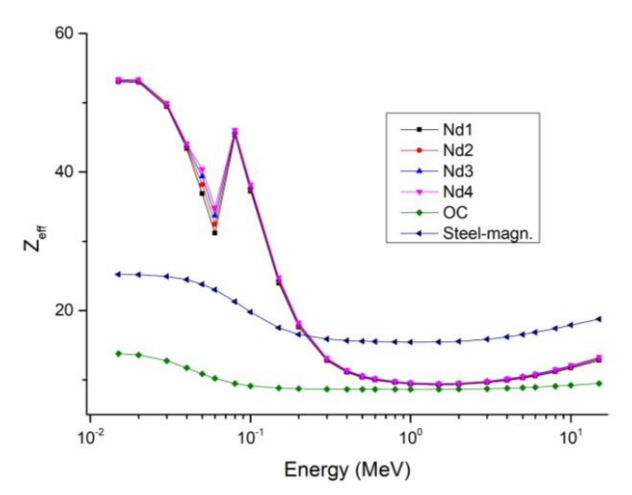


Figure 6. Variations of values of the Zeff (a) and Zeq (b) versus energies.



**Figure 7.** The comparative results of the Zeff for the samples and shields reported before.

In conclusion, the proportionality between Neff and Ceff of the glasses is evident. The variations in Neff and Ceff results with energies are demonstrated in Figs. 8(a-b), respectively. Alhough the values are seen very close, it becomes evident that Nd4 is characterised by the highest Neff and Ceff results especially at low energies among the glasses. The maximum measured values for Ceff, Zeff, and Neff at  $\approx$  70 keV may be assigned to the K-absorption edge of the W element (Aygun et al. 2023).

To define the EBF and EABF of glasses with respect to 16 penetration depths, the utilization of Phy-X/PSD proved instrumental. The subsequent figures, 9 and 10, illustrate the alterations in these parameters with regard to the incident energy. In the PE region, all energies result in the absorption of lower energy photons, leading to a relatively minor buildup. However, a considerable scattered photons number in the region of CS can facilitate a notable accumulation of photons, thereby reaching peak values in the mid-energy region. It is

obtained that the rate of photon absorption within the PP region is relatively high, leading to lower BUFs in the higher energy levels. The findings suggest that the photon clustering for Nd4 is greater than that observed in the remaining glasses, as demonstrated by the EBF and EABF values determined. In addition, the increases at  $\approx 70 \text{ keV}$  may be explained as absorption in the K-edge of W.

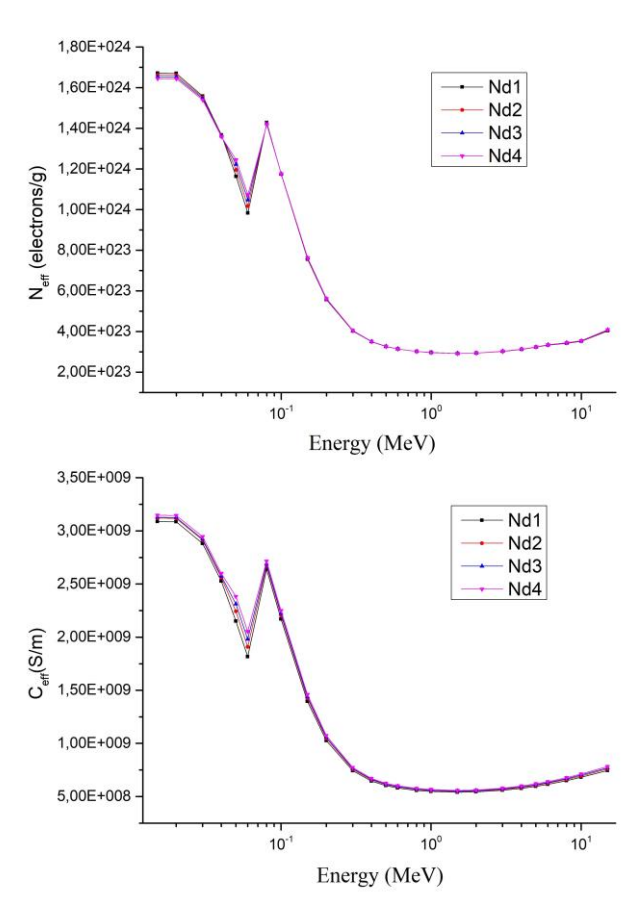


**Figure 8.** Dependence of Neff (a) and Ceff (b) values versus photon energies.

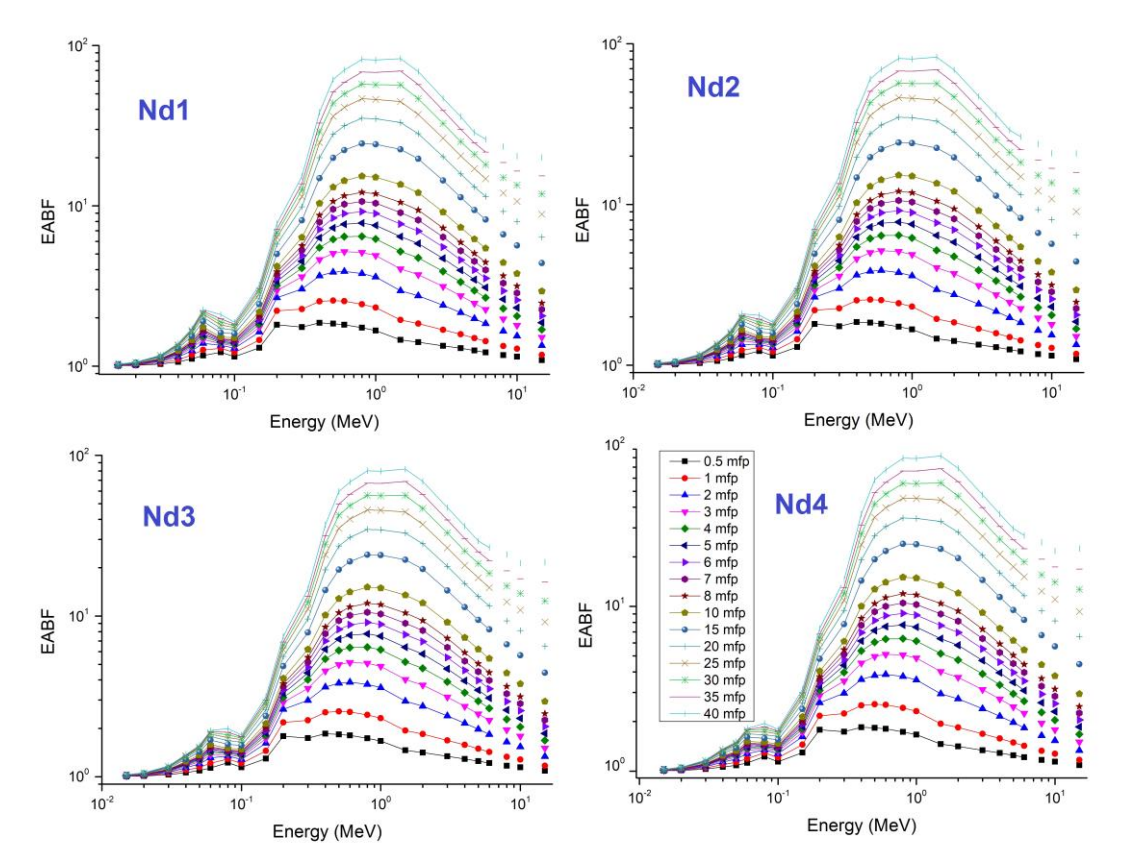


Figure 9. Dependence of EABF values versus photon energies.

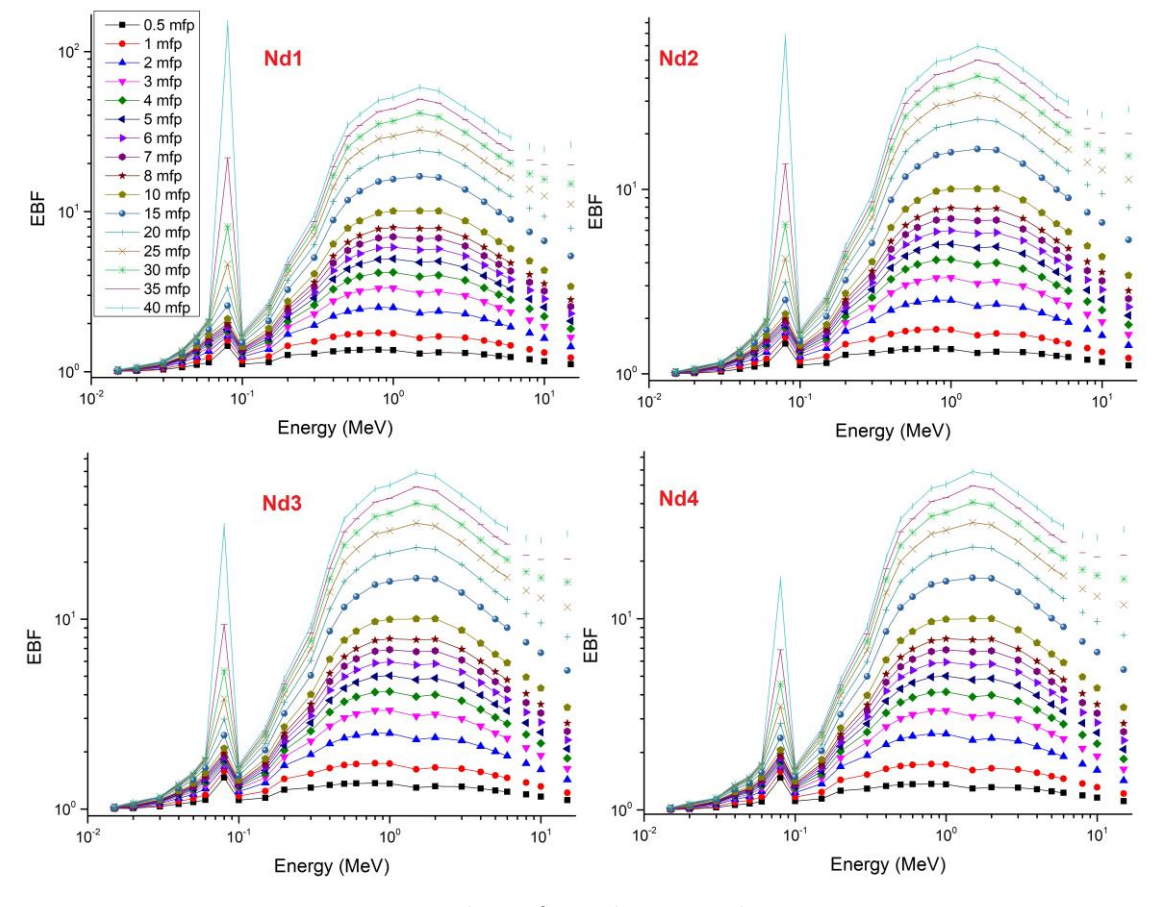


Figure 10. Dependence of EBF values versus photon energies.

The  $\mu en/\rho$  values are calculated and displayed in Fig. 11 (a). The findings are in the range of 0.017830- 1508.236, 0.017961 - 1540.168, 0.018088 - 1571.536 and 0.018215 - 1602.610 for Nd1, Nd2, Nd3 and Nd4, respectively. The findings follow this order: Nd1 < Nd2 < Nd3 < Nd4. The values of KERMA are estimated and presented in Fig. 11 (b). The values of KERMA are minimum for low energies, and then rise and achieve the maximum at 0.04 MeV. Finally, they showed an abrupt decrease, subsequently followed by a period of unremarkable behaviour. Nd4 has the biggest KERMA at 0.04 MeV wheras Nd1 has the least.

The neutron shielding effectiveness of the glasses is evaluated through the analysis of their FNRCS values, as illustrated in Fig. 12. Nd4 exhibits the highest value for fast neutrons, while Nd1 displays the least effective result. The FNRCS values are assessed in comparison with a selection of shielding materials, including bizmuth (Bi20) glass, graphite and borogypsum (BG), ytterbium (Yb2.5) as documented in previous studies (Kaky et al. 2024; Aygun et al. 2024; Al-Buriahi et al. 2020; Aygun and Aygun 2023).

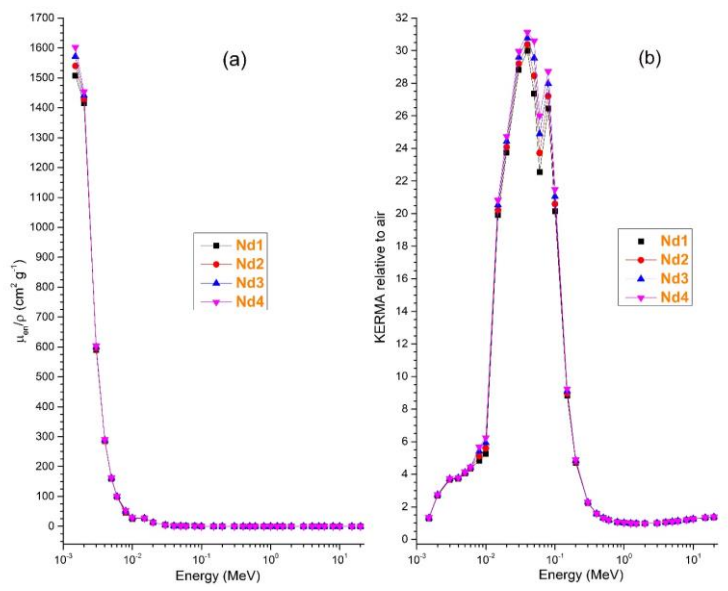
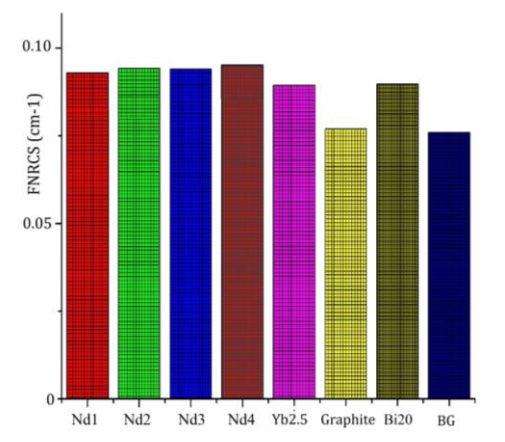


Figure 11. Changes of the values of  $\mu en/\rho$  (a) and KERMA (b) versus energies.



**Figure 12.** FNRCS values of the glasses in comparison to other materials studied before.

It is imperative to consider the interaction of CPs with glasses when developing radiation therapy protocols. To this end, the MSP values of for the glasses in question were estimated, and the findings are graphed in the range of  $10^{-2}$ - $10^3$  MeV and given in Fig. 13. The MSPVs of electrons demonstrate a decline with rising energy levels, subsequently exhibiting a gradual ascension. In this instance, the process by which electrons lose energy is considered. It is hypothesised that electrons undergo

bremsstrahlung and Coulomb interactions. The MSP values for electrons (5x10<sup>-5</sup>-10<sup>3</sup> MeV) are among 1.472 -281.364, 1.469 - 279.429, 1.467 - 277.837 and 1.465 -276.130 for Nd1, Nd2, Nd3 and Nd4, respectively. MSP values for positrons are among 1.432 - 425.196, 1.430 -422.537, 1.427 - 420.256 and 1.425 - 417.856 for Nd1, Nd2, Nd3 and Nd4, respectively. MSP values for electron and positron particles, the energy increases, the value gradually decreases and eventually reaches the maximum value. The MSP results of proton are among 1.742 -506.092, 1.738 - 503.288, 1.735 - 500.484 and 1.731 -497.780 for Nd1, Nd2, Nd3 and Nd4, respectively. For alpha particles, the MSP value demonstrates an initial rise in energy levels, which is followed by a subsequent decline. The MSPVs of alpha particles are among 12.213 -1434.29, 12.183 - 1426.281, 12.163 - 1418.415 and 12.133 - 1411.264 for Nd1, Nd2, Nd3 and Nd4, respectively. It should be highlighted that the manner in which alpha particles and protons behave can be influenced by the dependency of their nuclear and electronic energy losses. The following order of MSPVs for the glasses are obtained for the CPs: MSPalpha > MSPprotons > MSPpositrons > MSPelectrons..

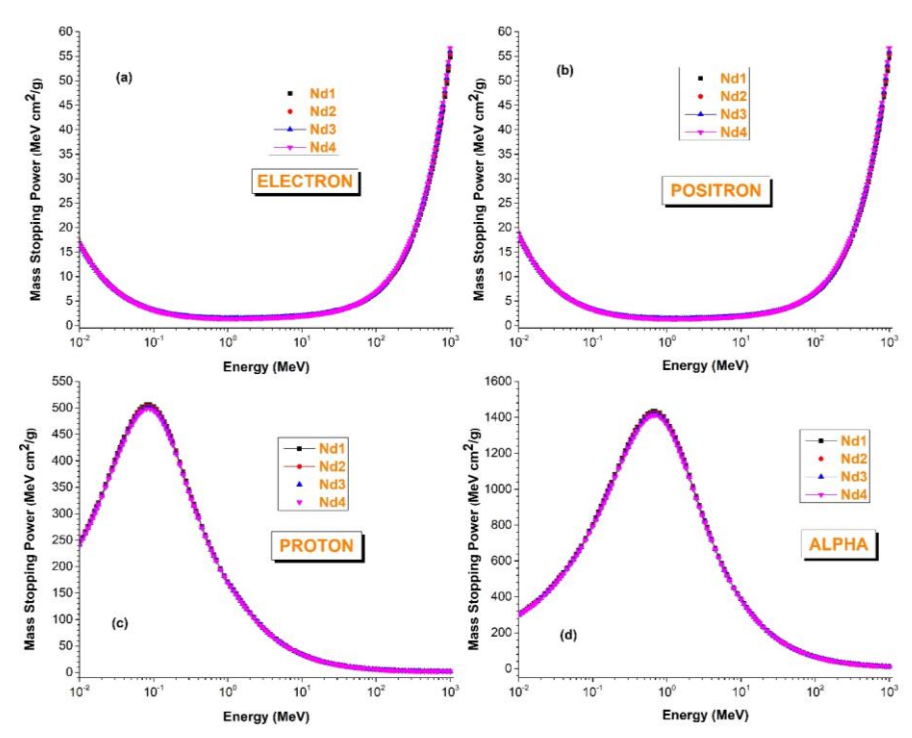


Figure 13. Changes of MSPVs of electron, proton, positron and alpha particles versus energy.

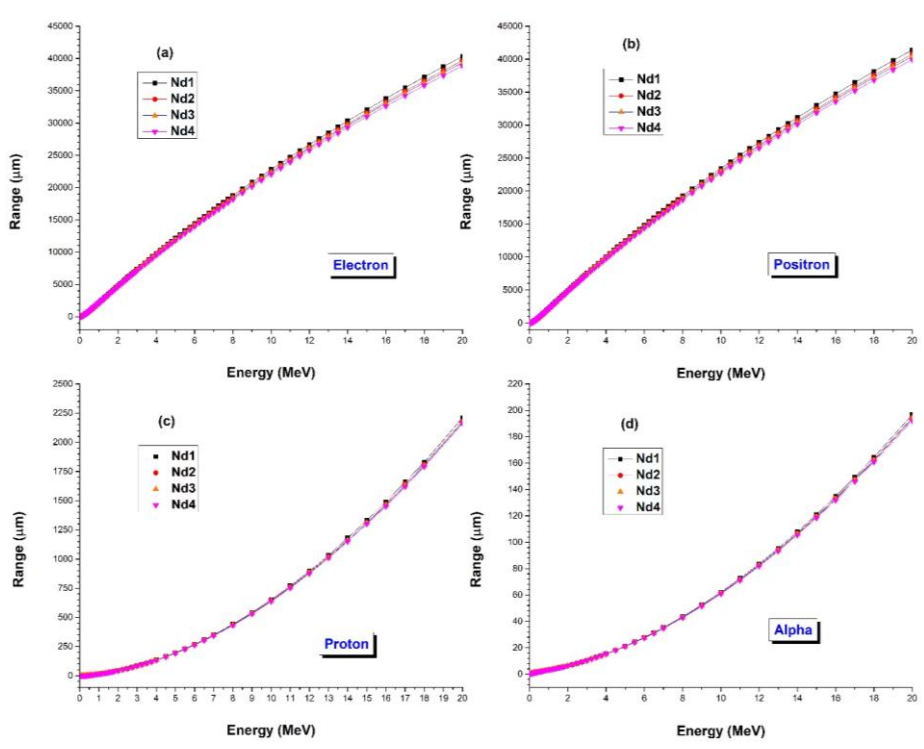
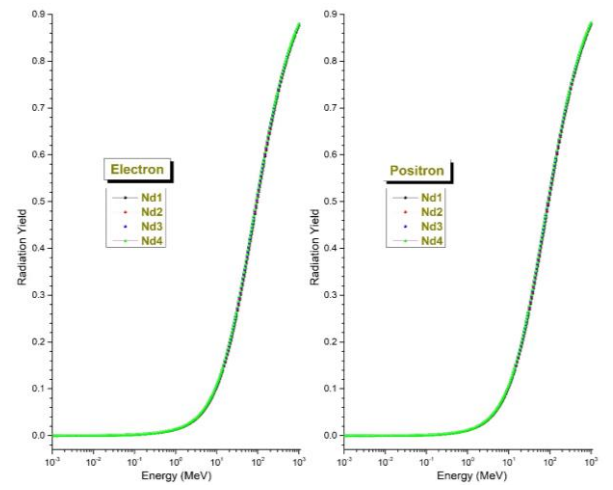


Figure 14. Variations of Rp of electron, positron, proton and alpha particles.

The Rp findings are determined by SRIM and PENELOPE codes, and are displayed (0-20 MeV) in Fig. 14. For electron, the Rp values ( $5 \times 10^{-5} - 10^3$  MeV) are among 1.341 -40317, 1.325 - 39672, 1.320 - 39337 and 1.1309 - 38864 for Nd1, Nd2, Nd3 and Nd4, respectively. For positrons, the Rp results are among 1.192 - 41405, 1.177 - 40745, 1.172 - 40404 and 1.162 - 39923 for Nd1, Nd2, Nd3 and Nd4, respectively. For proton, the Rp results are among 0.1545 - 2210, 0.1526 - 2180, 0.1519 - 2170 and 0.1506 - 2160 for Nd1, Nd2, Nd3 and Nd4, respectively.

For alpha, the Rp results are among 0.0963 - 196, 0.0951 - 194, 0.0947 - 193 and 0.0939 - 192 for Nd1, Nd2, Nd3 and Nd4, respectively. The Rp values are placed in the following manner: Rpalpha < Rpproton < Rpelectron < Rppositron. In addition, for CPs, the Rp values are in the following order: Nd1 > Nd2 > Nd3 > Nd4. It should be stated that there is an obvious inverse relationship between glass density and Rp value, the sample given by the biggest density exhibiting a shorter Rp and the lowest density sample exhibiting a greater Rp.

The radiation yield (Ry) values for the glasses have been determined by the PENELOPE code at the range of energies 0.001-1000 MeV, and the results have been displayed in a plot (see Fig. 15). In this regard, the Ry values for electrons are among 0.00001882 - 0.8761, 0.00001894 - 0.8773, 0.00001906 - 0.8785 and 0.00001918 - 0.8796 for Nd1, Nd2, Nd3 and Nd4, respectively. The Ry values for positrons are among 0.000002382 - 0.8782, 0.000002377 - 0.8794, 0.000002373 - 0.8806 and 0.000002368 - 0.8817 for Nd1, Nd2, Nd3 and Nd4, respectively. Based on these findings, it can be noted that the Ry values of glasses for electron and positron the following sequence is given as Nd4 > Nd3 > Nd2 > Nd1.



**Figure 15**. The changes of Ry values of electron and positron with energy.

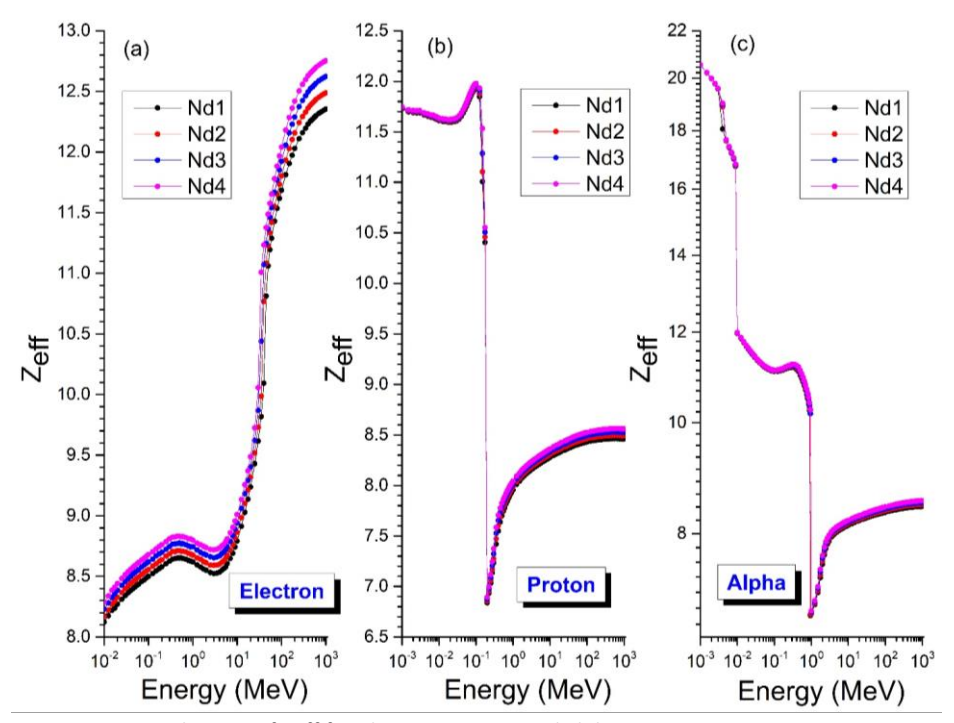


Figure 16. Changes of Zeff for electron, proton and alpha interactions versus energy.

The Zeff outcomes of the samples for the CPs are displayed in Fig. 16. For electron, the Zeff data are between 8.122 – 12.354, 8.170 – 12.487, 8.228 – 12.623 and 8.283 - 12.753 for Nd1, Nd2, Nd3 and Nd4, respectively. For proton, the Zeff values are among 8.360 - 11.924, 8.394 - 11.943, 8.428 - 11.961 and 8.461 -11.978 for Nd1, Nd2, Nd3 and Nd4, respectively. For alpha, the Zeff results are among 8.455 - 20.540, 8.487 -20.541, 8.519 - 20.543 and 8.551 - 20.545 for Nd1, Nd2, Nd3 and Nd4, respectively. The Zeff data for the samples associated with the CPs are presented in the subsequent sequence: Nd1 < Nd2 < Nd3 < Nd4. The Zeff values for electrons demonstrate a progressive enhancement in tandem with the rising kinetic energy for each individual glass. It has been evidenced that the behavior of alpha particles and protons exhibits a non-monotonic variation

in both high and low energy contents. Moreover, Zeff data have been observed to rise in conjunction with rising density of glass.

Additionally, for the CPs, the glasses Neff results are computed and illustrated in Fig. 17. For electron, the Neff results are changed between 2.553 x  $10^{23} - 3.930 \times 10^{23}$ . For proton, the Neff values are varied between  $2.608 \times 10^{23} - 3.761 \times 10^{23}$ . For alpha, the Neff values are changed between  $2.110 \times 10^{23} - 6.478 \times 10^{23}$ . A comparable pattern is evident for electrons' Neff values as Zeff, which demonstrate a gradual increase in correlation with the rise in kinetic energy for every individual glass. It is notable that the Neff values for alpha and proton exhibit non-monotonic variations in both the low and high energies.

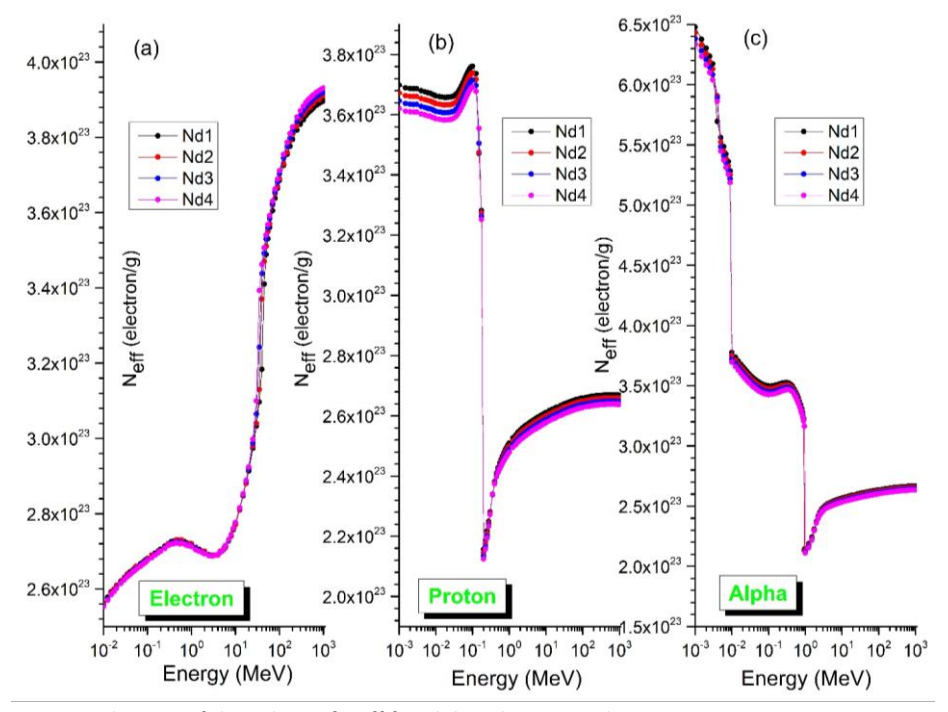
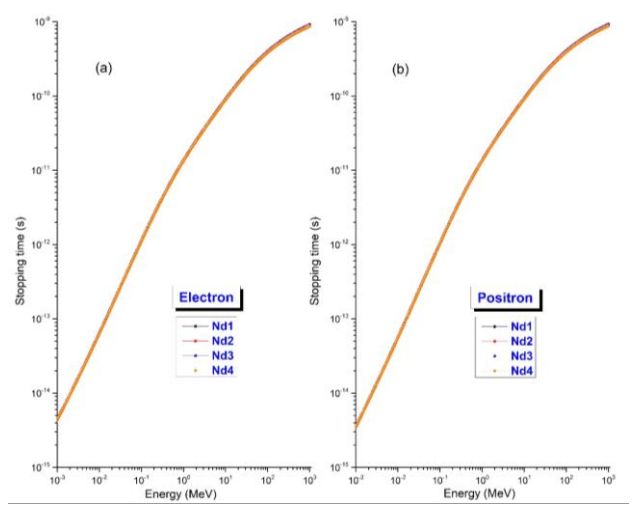


Figure 17. Changes of the values of Neff for alpha, electron and proton interactions versus energy.

Also, the stopping time (St) findings of the glasses for electrons and positrons are computed and illustrated (10-<sup>3</sup>-10<sup>3</sup> MeV) in Fig. 18. In this regard, for electrons, the St values are among  $9.575 \times 10^{-15} - 9.157 \times 10^{-10}$ ,  $9.466 \times 10^{-10}$  $^{15}$  – 8.946 x  $10^{-10}$ , 9.971 x  $10^{-15}$  – 8.809 x  $10^{-10}$  and 9.896 x  $10^{-15} - 8.645 \times 10^{-10}$  for Nd1, Nd2, Nd3 and Nd4, respectively. The St values for positrons are among 9.933  $\times 10^{-15} - 9.246 \times 10^{-10}$ , 9.819  $\times 10^{-15} - 9.033 \times 10^{-10}$ , 9.782  $\times 10^{-10}$  $10^{-15} - 8.896 \text{ x } 10^{-10} \text{ and } 9.708 \text{ x } 10^{-15} - 8.731 \text{ x } 10^{-10} \text{ for }$ Nd1, Nd2, Nd3 and Nd4, respectively. In light of the results, it has been documented that the St value increases in conjunction with an increase in energy for electron and positrons. The largest St values follow the following order: Stpositron > Stelectron. Also, the largest St values of the glass is given in the following sequence: Nd1 > Nd2 > Nd3 > Nd4.



**Figure 18.** Deviations of the St of electron and positron particle as a function of energy.

### 4. Conclusions

In the study, the radiation attenuation performances of the glasses added by Nd3+ with the components of [(65x) B2O3 - 5Al2O3 - 20Na2O - 10WO3 - xNd2O3] x = zero,0.25, 0.50 and 0.75 mol% were analyzed for fast neutron, gamma-ray and CPs by PENELOPE, Phy-X/PSD, SRIM and PAGEX softwares. The LACVs, MACVs, MFPVs, HVLVs, Zeff, ACS and ECS data were investigated and it was noted that the parameters displayed a behaviour depending on the energy, as a result of processes by which photons interact operating across a wide range of energies. The maximum and minimum values for the following parameters, LACVs, MACVs, ECS, ACS, µen/p and Zeff, were identified for Nd4 and Nd1 while those of HVLVs and MFPVs were obtained for Nd1 and Nd4, respectively. The glass in which the greatest FNRCS value, Nd4, was found to exhibit the optimal neutron shielding properties. This suggests that this is the glass by the best effective neutron attenuating capability. The MSP findings of the samples, ordered from highest to lowest, are as follows: alpha, proton, positron, electron. The glass comprising the Nd1 composition exhibited maximal Rp values for CPs, whereas the glass comprising the Nd4 composition exhibited the minimal values. The investigation revealed that the addition of Nd3+ to the glasses in question resulted in an enhanced ability to shield against an array of CPs. The findings of the study indicated that Nd4 exhibited the highest degree of shielding efficacy against gamma rays, CPs, and neutrons whereas Nd1 exhibited the least one. It can be postulated that the glass with a greater concentration of Nd3+ provides enhanced

radiation attenuation, whereas those with a lower concentration of Nd³+ offer a comparatively reduced level of attenuation. Consequently, it can therefore be concluded that glasses activated by Nd3+ and comprising a composition of (65-x) B2O3 - 5Al2O3 - 20Na2O -10WO3 - xNd2O3 are suitable as shields in a diverse array of applications. The findings indicate that the examined glasses with higher Nd<sup>+3</sup> content may exhibit exceptional radiation attenuation characteristics, rendering them a candidate for radiation protecting applications. The process of attenuation in REE doped glasses is an important factor in the development of efficient shielding, which make them suitable for use in radiological procedures and technologies of lighting. In the field of radiation shielding, the transparency of glass constitutes a critical advantage, rendering the material suitable for specific applications. These include the fabrication of masks designed to safeguard the face and other anatomical regions during radiological procedures, as well as the utilisation of fenestration and wall surfaces in radiography rooms. Therefore, it may be proposed that Nd3+-doped glasses will be of significant benefit in advancing materials science.

### **Declaration of Ethical Standards**

The authors declare that they comply with all ethical standards.

### **Credit Authorship Contribution Statement**

- Author-1: Conceptualization, Methodolog, Validation, Formal analysis,
  Writing original draft, Writing review and editing,
  Visualization, Supervision.
- Author-2: Conceptualization, Methodolog, Validation, Formal analysis, Writing original draft, Writing review and editing, Visualization, Supervision.

### **Declaration of Competing Interest**

The authors state there is no known competing interest.

### Data Availability

The data can be available on request.

### References

- Abouhaswa, A.S., Taha, T.A.M. 2024. Synthesis, optical and magnetic properties of Nd2O3/borate strontium fluoride glasses. Ceram. Int, 50(7), 11032-11039. https://doi.org/10.1016/j.ceramint.2024.01.004.
- Al-Buriahi, M., Abouhaswa, A., Tekin, H., Sriwunkum, C., El-Agawany, F., Nutaro, T. et al. 2020. Structure, optical, gamma-ray and neutron shielding properties of NiO doped B2O3–BaCO3–Li2CO3 glass systems. Ceram. Int. 46, 1711–1721. https://doi.org/10.1016/j.ceramint.2019.09.144
- Aljewaw, O.B., Abdul Karim, M.K., Kamari, H.M., Mohd Zaidet, M.H. et al. 2022. Physical and spectroscopic characteristics of lithiumaluminium-borate glass: effects of varying Nd2O3 doping contents. J. Non-Cryst. Solids, 575, 121214.

- https://doi.org/10.1016/j.jnoncrysol.2021.121214
- Alsafi, K., Ismail, Y.A.M., Aloraini, D.A., Almutairi, H.M., Al-Saleh, W.M., Shaaban, Kh S. 2024. Exploring the radiation shielding properties of B2O3-SiO2-ZnO-Na2O-WO3 glasses: A comprehensive study on mechanical, gamma, and neutron attenuation characteristics. Progress Nucl. Energy, 170, 105151, https://doi.org/10.1016/j.pnucene.2024.105151.
- Alzahrani, F.M.A., Alfryyan, N., Alrowaili, Z.A. et al. 2024. Gamma Shielding and Dosimetry Parameters of Sodium-Silicate Glasses with Significant Role of TbF3 Addition. Silicon 16, 2037–2047. https://doi.org/10.1007/s12633-023-02813-9
- ANSI/ANS 6.4.3 1991. Gamma-ray Attenuation Coefficients and Buildup Factors for Engineering Materials. American Nucl Soc, La Grange Park, Illinois.
- Attallah, M., Farouk, M., Samir, A. 2024. Optimize the structural, optical, and thermal properties of Nd3+ ions doped boro-aluminum-tungsten glass. Ceram. Int, 50, 9528–9534. https://doi.org/10.1016/j.ceramint.2023.12.271
- Aygun, M., Aygun. Z. 2023. A comprehensive analysis on radiation shielding characteristicsof borogypsum (boron waste) by Phy-X/PSD code. Revista Mexicana de Fisica, 69, 1–7. https://doi.org/10.31349/RevMexFis.69.040401
- Aygun, M., Aygun, Z., Ercan E. 2023. Radiation protection efficiency of newly produced W-based alloys: Experimental and computational study. Radiat. Phys. Chem. 212, 111147. https://doi.org/10.1016/j.radphyschem.2023.111147
- Aygun, M., Aygun, Z., Han, I., Han, E.N. 2024. Theoretical investigation for ytterbium effect on radiation shielding characteristics of 50Bi2O3-15Li2O-15PbO-(20-x)B2O3-YB2O3 borate glasses. Konya J. Engineer. Sci., 12(3), 737-755. https://doi.org/10.36306/konjes.1496688
- Aygun, M., 2024. Gamma-ray, fast neutron and charged particle shielding performance of 15Li2O-25BaO-(40-x)B2O3-20P2O5-xDy2O3 glass system. Radiat. Phys. Chem., 219, 111671. https://doi.org/10.1016/j.radphyschem.2024.111671
- Bashter, I.I. 1997. Calculation of radiation attenuation coefficients for shielding concretes. Annl. Nucl. Energy, 24, 1389-1401. https://doi.org/10.1016/S0306-4549(97)00003-0
- Baykal, D.S., Almisned, G., Alkarrani, H., Tekin, H. O. 2024. Exploring gamma-ray and neutron attenuation properties of some high-density alloy samples through MCNP Monte Carlo code. Inter. J. Comput. Experiment. Sci. Engineer. 10(3), 470-479. https://doi.org/10.22399/ijcesen.422
- Biradar, S., Chandrashekara, M.N., Dinkar, M.A. 2024. Synergistic optimization of physical, thermal,

- structural, mechanical, optical and radiation shielding characteristics in borate glasses doped with Bi2O3. Optical Mater., 155, 115815. https://doi.org/10.1016/j.optmat.2024.115815
- Boussetta, A., Al-Syadi, A.M., Damak, K., Ersundu, A.E., Çelikbilek, E.M, Ramadan, E., Alshehri, A.M., Hussein, K.I., et al. 2024. Investigation of Thermal and Spectroscopic Properties of Tellurite-Based Glasses Doped with Rare-Earth Oxides for Infrared Solid-State Lasers. Mater. (Basel). 17(15), 3717. https://doi.org/10.3390/ma17153717.
- Charfi, B., Herrmann, A., Zekri, M., Qasymeh, M., Damak, K., Maâlej, R. 2024. Correlation of rare earth coordination and spectral properties in Er3+ doped Na2O–Al2O3–SiO2 glasses with different Al2O3 concentrations by molecular dynamics simulations. J. Luminescence, 273, 120676, https://doi.org/10.1016/j.jlumin.2024.120676.
- Gracie, P., Yasmin, J., Geetha, D. 2024. Structural and optical investigations of RE3+: Yb, Er, Sm, Nd, Cedoped multi-functional silica glasses for photonic applications. J. Physics D: Appl. Phys., 57, 205101. https://doi.org/10.1088/1361-6463/ad2834
- Han, I., Demir, L. 2009. Studies on effective atomic numbers, electron densities from mass attenuation coefficients in TixCo1-x and CoxCu1-x alloys. Nucl. Instr. Methods in Phys. Res. Section B, 267, 3505– 3510. https://doi.org/10.1016/j.nimb.2009.08.022
- Harima, Y. 1993. An historical review and current status of buildup factor calculations and applications. Radiat. Phys. Chem. 41, 631–672.
- Harima, Y., Sakamoto, Y., Tanaka, S., Kawai, M. 1986. Validity of the Geometric-Progression Formula in Approximating Gamma-Ray Buildup Factors. Nucl. Sci. Engineer., 94, 24–35.
- Kaewnum, E., Wantana, N., Kaewkhao, J. 2018. Luminescence study and Judd-Ofelt analysis of Nd3+ doped lithium lanthanum borate glass for green laser device. Mater. Today: Proc. 5(6), 13954–13962.
- Kaky, K.M., Sayyed, M.I., Hamad, M.K., Biradar, S., Mhareb, M.H.A., Altimari, U., Taki, M.M. 2024. Bismuth Oxide Effects on Optical, Structural, Mechanical, and Radiation Shielding Features of Borosilicate glasses. Optical Mater. 155, 115853. https://doi.org/10.1016/j.optmat.2024.115853.
- Karpuz, N. 2024. Effective Atomic Numbers of Glass Samples. Inter. J. Comput. Experiment. Sci. Engineer. 10(2), 236-240. https://doi.org/10.22399/ijcesen.340
- Kutu, N. 2024. Neutron Shielding Properties of Cellulose Acetate CdO-ZnO Polymer Composites. Inter. J. Comput. Experiment. Sci. Engineer. 10(2). https://doi.org/10.22399/ijcesen.322

- L'Annunziata, M.F. 2003. Nuclear Radiation, Its Interaction with Matter and Radioisotope Decay. Handbook of Radioactivity Analysis, 1-122.
- Lakshminarayana, G., Kumar, A., Tekin, H.O., Shams A.M. 2020. Binary B2O3–Bi2O3 glasses: scrutinization of directly and indirectly ionizing radiations shielding abilities. J. Mater. Res. Technol., 9(6), 14549-14567. https://doi.org/10.1016/j.jmrt.2020.10.019.
- Madhu, A., Al-Dossari, M., Kagola, U.K., Abd EL-Gawaad, N.S., Srinatha, N. 2024. Probing the structural and spectroscopic characteristics of Ag2O-modified Li2O–CaO–B2O3 glasses doped with Nd2O3. Ceram. Inter., 50(11), 20764-20776, https://doi.org/10.1016/j.ceramint.2024.03.205.
- Malchukova, E.V., Nepomnyashchikh, A.I., Boizot, B., Terukov, E.I. 2018. Radiation Effects and Optical Properties of Aluminoborosilicate Glass Doped with RE Ions. Glass Phys. Chem., 44(4), 356–363. https://doi.org/10.1134/S1087659618040090
- Manjunatha, H.C. 2017. A study of gamma attenuation parameters in poly methyl methacrylate and Kapton. Radiat. Phys. Chem., 137, 254–259. https://doi.org/10.1016/j.radphyschem.2016.01.024
- Mhareb, M.H.A. 2024. An investigation of the effects of Nd2O3 on the mechanical, structural, and optical properties of borosilicate glasses for optimizing radiation shielding performance. Optical Mater., 157, 116079.
  - https://doi.org/10.1016/j.optmat.2024.116079
- Matos, I.M., Balzaretti, N.M. 2024. Effect of mixed alkali ions on the structural and spectroscopic properties of Nd3+ doped silicate glasses. Results in Mater., 21, 100517. https://doi.org/10.1016/j.rinma.2023.100517.
- Nabil, I.M., El-Seidy, A.M.A., Mosleh, A.T. et al. 2024. Influence of low copper oxide additives on B2O3-Li2O-Na2O-CaO-SrO-As2O3 glasses: a physical, structural, and radiological study. J Mater Sci: Mater Electron, 35, 1329.
  - https://doi.org/10.1007/s10854-024-12891-z
- Prabhu, S., Jayaram, S., Bubbly, S.G., Gudennavar, S.B. 2021. A simple software for swift computation of photon and charged particle interaction parameters: PAGEX. Appl. Radiat. Isotopes, 176, 109903. https://doi.org/10.1016/j.apradiso.2021.109903
- Sakar, E., Özpolat, Ö.F., Alım, B., Sayyed, M.I., Kurudirek, M. 2020. Phy-X / PSD: Development of a user friendly online software for calculation of parameters relevant to radiation shielding and dosimetry. Radiat. Phys. Chem. 166, 108496.
  - https://doi.org/10.1016/j.radphyschem.2019.108496
- Sempau, F., Fernandez-Varea, J.M., Acosta, E., Salvat, F. 2023. Experimental benchmarks of the Monte Carlo code PENELOPE. Nucl. Instr. Methods B, 207, 107-123.

- https://doi.org/10.1016/S0168-583X(03)00453-1
- Sivakumar, T., Panjanathan, V., Dhinakaran, A.P. 2024. Predominance of Yb3+ and Ce3+ on the AlTaBaBO: Yb and BaTiSbBPO: Ce glasses for effective photoluminescence and radiation shielding properties towards w-LED and γ-ray shielding applications. Radiat. Phys. Chem., 224, 111995. https://doi.org/10.1016/j.radphyschem.2024.11199
- Yaacob, S.N.S., Sahar, M.R., Mohd-Noor, F., Shamsuri, W.N.W. et al. 2021. The effect of Nd2O3 content on the properties and structure of Nd3+ doped TeO2–MgO–Na2O-glass. Optical. Mater., 111, 110588. https://doi.org/10.1016/j.optmat.2020.110588.
- Yorulmaz, N., Yasar, M.M., Acikgoz, A., Kavun, Y., Demircan, G. 2024. Influence of Gd2O3 on structural, optical, radiation shielding, and mechanical properties of borate glasses, Optical Mater., 149, 115032, https://doi.org/10.1016/j.optmat.2024.115032
- Ziegler, J.F. SRIM-The Stopping and Range of Ions in Matter. http://www.srim.org.